

# Spin currents in diluted magnetic semiconductors (extended version)

S.D. Ganichev,<sup>1</sup> S.A. Tarasenko,<sup>2</sup> V.V. Bel'kov,<sup>2</sup> P. Olbrich,<sup>1</sup> W. Eder,<sup>1</sup> D.R. Yakovlev,<sup>2,3</sup>

V. Kolkovskiy,<sup>4</sup> W. Zaleszczyk,<sup>4</sup> G. Karczewski,<sup>4</sup> T. Wojtowicz,<sup>4</sup> and D. Weiss<sup>1</sup>

<sup>1</sup> *Terahertz Center, University of Regensburg, 93040 Regensburg, Germany*

<sup>2</sup> *A.F. Ioffe Physico-Technical Institute, Russian Academy of Sciences, 194021 St. Petersburg, Russia*

<sup>3</sup> *Experimental Physics 2, TU Dortmund University, 44221 Dortmund, Germany, and*

<sup>4</sup> *Institute of Physics, Polish Academy of Sciences, 02-668 Warsaw, Poland*

(Dated: February 3, 2022)

Spin currents resulting in the zero-bias spin separation have been observed in unbiased diluted magnetic semiconductor structures (Cd,Mn)Te/(Cd,Mg)Te. The pure spin current generated due to the electron gas heating by terahertz radiation is converted into a net electric current by application of an external magnetic field. We demonstrate that polarization of the magnetic ion system enhances drastically the conversion due to the spin-dependent scattering by localized Mn<sup>2+</sup> ions and the giant Zeeman splitting.

PACS numbers:

The generation of spin currents in low-dimensional semiconductor structures recently attracted a great attention. Pure spin currents represent equal and oppositely directed flows of spin-up and spin-down electrons. By that the net electric current is zero. Spin currents lead to a spatial spin separation and, consequently, an accumulation of the oppositely oriented spins at the edges of the sample. Spin currents in semiconductors can be generated by an electric field, like in the spin Hall effect (for review see [1, 2]) as well as by optical means under interband optical transitions in non-centrosymmetric bulk and low-dimensional semiconductors [3, 4, 5]. They can also be achieved as a result of zero-bias spin separation, e.g. by electron gas heating followed by spin-dependent energy relaxation of carriers [6]. So far in low-dimensional semiconductors pure spin currents have been reported for non-magnetic structures only. However, spin-dependent effects can be greatly enhanced by exchange interaction of electrons with magnetic ions in diluted magnetic semiconductors (DMS) like, e.g. (Cd,Mn)Te [1, 7, 8, 9]. Moreover, the strength of these effects can be widely tuned by temperature, magnetic field and concentration of the magnetic ions.

Here we report on the observation of the zero-bias spin separation in (Cd,Mn)Te/(Cd,Mg)Te QWs with Mn<sup>2+</sup> magnetic ions. We demonstrate that absorption of terahertz (THz) radiation leads to a pure spin current. The effect is investigated in an external magnetic field converting the spin separation into a net electric current. The application of a magnetic field to DMS structures results in the giant Zeeman spin splitting as well as in the spin-dependent exchange scattering of electrons by magnetic impurities. Both effects disturb the balance of the oppositely directed spin-polarized flows of electrons yielding an electric current. We demonstrate that the spin-dependent exchange scattering of electrons by magnetic impurities plays an important role in the current generation providing a handle to manipulate the spin-

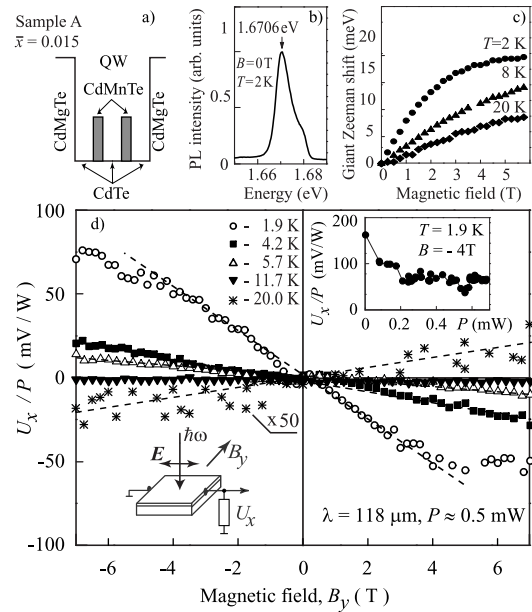


FIG. 1: (Cd,Mn)Te/(Cd,Mg)Te QW with  $\bar{x} = 0.015$  (sample A). (a) Sketch of the structure. (b) Photoluminescence spectrum. (c) Shift of the PL line corresponding to 1/2 of the total giant Zeeman splitting. (d) Magnetic field dependence of the voltage signal  $U_x$  normalized by the radiation power  $P$  in response to a low excitation power applying *cw* laser. Insets show the experimental geometry (left, bottom) and  $U_x/P$  as a function of the radiation power obtained at  $B = -4$  T (right, up).

polarized currents.

We study spin currents on (Cd,Mn)Te/(Cd,Mg)Te single QW structures grown by molecular beam epitaxy on (001)-oriented GaAs substrates [10, 11, 12]. The quantum wells were grown by a digital alloy technique [13], i.e. by inserting evenly spaced thin layers of Cd<sub>1-x</sub>Mn<sub>x</sub>Te during the growth of 10 nm wide CdTe-based QW [Fig. 1(a)]. Two DMS samples were fabricated: Sample A with two insertions of Cd<sub>0.8</sub>Mn<sub>0.2</sub>Te

TABLE I: Sample parameters. Here electron mobility,  $\mu$ , and electron concentration,  $n_e$ , in the QW was evaluated from transport experiments and  $\bar{x}$  is the effective average concentration of Mn, determining the electron spin splitting, which was estimated from the giant Zeeman shift of interband emission line [Fig. 1(c)].

| sample | $x$  | $\bar{x}$ | $\mu$ at 4.2 K<br>cm <sup>2</sup> /Vs | $n_e$ at 4.2 K<br>10 <sup>11</sup> cm <sup>-2</sup> | $E_F$<br>meV |
|--------|------|-----------|---------------------------------------|---|--------------|
| A      | 0.20 | 0.015     | 9500                                  | 4.7   | 11.7         |
| B      | 0.14 | 0.013     | 16000                                 | 6.2   | 15.4         |
| C      | 0    | 0         | 59000                                 | 4.2   | 10.4         |

and a nominal thickness of three monolayers and sample B with three single monolayers of Cd<sub>0.86</sub>Mn<sub>0.14</sub>Te. The samples were modulation doped with Iodine donors introduced in a top Cd<sub>0.76</sub>Mg<sub>0.24</sub>Te barrier in a 15 nm distance from the QW. As a reference structure we use sample C without Mn insertion. The samples are characterized by transport measurements and optical spectroscopy. The photoluminescence (PL) spectrum of sample A shown in Fig. 1(b) is typical for modulation-doped QWs [14]. The linewidth of 11 meV corresponds to the Fermi energy,  $E_F$ , and is in good agreement with the transport measurements. In external magnetic fields this line shows a strong spectral shift to low energies, reflecting the giant Zeeman splitting of the band states in DMS [8]. This shift, shown in Fig. 1(c), is strongly temperature dependent and is about 2.5 times larger than the giant Zeeman splitting of the conduction band states. The samples parameters are summarized in Table I. For the photocurrent experiments square shaped ( $5 \times 5$  mm<sup>2</sup>) specimens with a pair of ohmic contacts centered on the sample edges along the direction  $x \parallel [1\bar{1}0]$  were prepared [see inset in Fig. 1(d)].

To generate spin photocurrents we heat an electron gas applying radiation of a low power continuous-wave (*cw*) optically pumped CH<sub>3</sub>OH laser operating at a wavelength  $\lambda = 118$   $\mu$ m and a power  $P \approx 0.5$  mW reaching the sample. In addition we used a high power pulsed NH<sub>3</sub> laser providing 100 ns pulses with  $\lambda = 148$   $\mu$ m and  $P$  up to 40 kW [15]. THz radiation with photon energies  $\hbar\omega \approx 10$  meV is chosen to induce only free carrier absorption. The radiation is linearly polarized with the polarization vector aligned along the  $x$ -axis. An in-plane magnetic field  $\mathbf{B} \parallel y$  (up to 7 T) is used to align the Mn<sup>2+</sup> spins and to convert the spin current into a spin-polarized charge current. The geometry of the experiment is sketched in the inset of Fig. 1(d). The photocurrent is generated at normal incidence of radiation in (001)-oriented unbiased devices and measured perpendicularly to the magnetic field. This experimental configuration excludes other effects known to cause photocurrents [6]. The radiation of the *cw* laser is modulated at 225 Hz. A photocurrent is measured across the 1 M $\Omega$

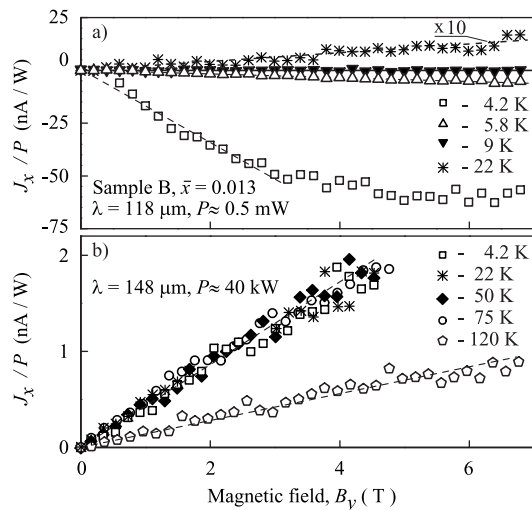


FIG. 2: Magnetic field dependence of the photocurrent  $J_x$  normalized by the radiation power  $P$  measured in sample B with  $\bar{x} = 0.013$ . a) Low power excitation ( $P \approx 0.5$  mW) with radiation of the *cw* laser b) High power excitation ( $P \approx 40$  kW) with radiation of the pulsed laser [16].

load resistance and recorded after 100 times voltage amplification by a lock-in amplifier. Whereas, in response to the pulsed radiation it is measured by the voltage drop across a 50  $\Omega$  load resistor.

Irradiating the DMS sample A with low power *cw* THz radiation we observe a voltage signal,  $U_x$ , for non-zero magnetic fields [Fig. 1(d)]. The signal polarity reverses with the change of the magnetic field direction. The signal is detected in a temperature range from 1.9 to 20 K. As an important result we observe that a cooling of the sample changes the signal sign and increases its absolute values by more than two orders of magnitude. While at moderate temperatures the signal depends linearly on  $B$ , at low  $T$  we observed a saturation of the photocurrent with rising magnetic field strength [see the data for  $T = 1.9$  K in Fig. 1(d)]. Similar results are obtained for sample B [Fig. 2(a)]. Both temperature and magnetic field dependences are typical for magnetization of DMS due to polarization of the Mn spin system in an external magnetic field.

Our experiments demonstrate that THz radiation induced photocurrent in DMS is controlled by the exchange interaction of electrons with Mn<sup>2+</sup> ions. The well-known effect of the exchange interaction is the giant Zeeman splitting [8], also detected in our samples by PL measurements [see Fig. 1(c)]. At low temperatures the exchange spin splitting overcomes the intrinsic one. The energy separation of the spin-up and spin-down electron subbands in (Cd,Mn)Te reads [8, 13]

$$E_Z(B) = g_e \mu_B B + \bar{x} S_0 N_0 \alpha B_{5/2} \left( \frac{5 \mu_B g_{Mn} B}{2 k_B (T_{Mn} + T_0)} \right), \quad (1)$$

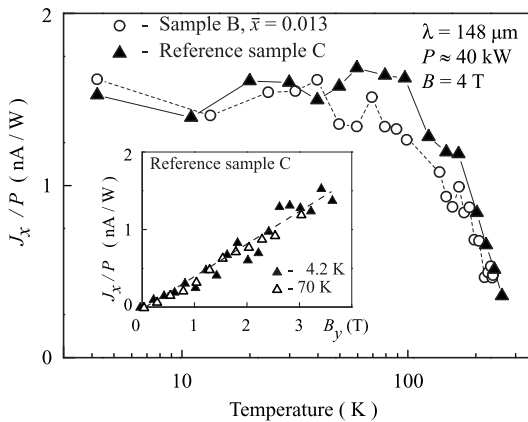


FIG. 3: Temperature dependence of the normalized photocurrent  $J_x/P$  excited by the radiation of  $\lambda = 148 \mu\text{m}$  at high excitation power of about 40 kW. Results are plotted for the sample B ( $\bar{x} = 0.013$ ) and the reference sample C. The inset shows the magnetic field dependence of the photocurrent for sample C.

where  $k_B$  is the Boltzmann constant and  $\mu_B$  the Bohr magneton. Here the first term stands for the intrinsic spin splitting with the electron  $g$ -factor ( $g_e = -1.64$  [17]). The second term is caused by exchange and contributed by the  $\text{Mn}^{2+}$   $g$ -factor ( $g_{\text{Mn}} = 2$ ) and the temperature of the Mn-spin system  $T_{\text{Mn}}$ . Phenomenological parameters  $S_0$  and  $T_0$  allow one to account for the Mn-Mn antiferromagnetic interactions within the magnetic ion system.  $B_{5/2}(\xi)$  is the modified Brillouin function of the argument in the brackets,  $N_0\alpha = 220 \text{ meV}$  is the exchange integral for conduction band electrons and  $N_0$  is the number of cations per unit volume.

It follows from Eq. (1) that the Zeeman splitting has a strong temperature dependence and reverses its sign due to opposite signs of  $g_e$  and  $N_0\alpha$ . This explains the sign inversion of the photocurrent in Fig. 1(d). However, while the photocurrent at  $T = 20 \text{ K}$  already changes its direction compared to lower temperatures [Fig. 1(d)] the sign of the Zeeman splitting, detected by PL, remains the same [Fig. 1(c)]. We attributed this fact to the heating of the  $\text{Mn}^{2+}$  spin system over the lattice temperature. Such an effect has been reported for DMS [18]. To check this assumption we investigate the power dependence of the signal. The inset of Fig. 1(d) demonstrates that at higher power the normalized signal decreases, indicating a reduction of the exchange effects due to an increase of  $T_{\text{Mn}}$ . To make the effect of heating more pronounced we applied the radiation of a pulsed THz laser with an eight orders of magnitude higher power than that of the *cw* laser. The data at low power and high power excitations are shown in Fig. 2 for sample B. We observe that the substantial increase of the radiation power results in the change of the signal polarity at  $T < 15 \text{ K}$ . Moreover, the drastic temperature dependence detected at low power excitation (Fig. 2(a)) in the range from 4.2

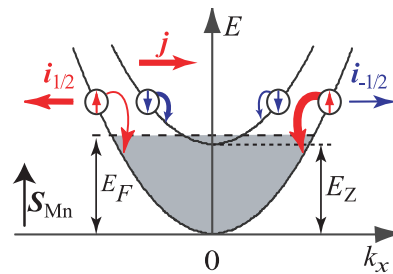


FIG. 4: Model of the zero-bias spin separation and conversion of the pure spin current into a net electric current due to an external magnetic field. The zero-bias spin separation is caused by the scattering assisted energy relaxation of the electron gas heated by radiation. The spin dependent part of the scattering matrix linear in  $\mathbf{k}$  and  $\sigma$  results in an asymmetric relaxation: transitions to positive and negative  $k'_x$ -states occur with different probabilities. This is indicated by bent arrows of different thickness. Thus, the transitions yield an asymmetric occupation of both subbands and hence electron flows. Without magnetic field these flows are oppositely directed and equal to each other. The Zeeman spin splitting causes a preferential occupation of one subband (the spin-up states in the figure) and disturbs the balance. As a result the pure spin current is converted into a spin polarized electric current. In DMS at low temperatures the conversion is amplified by the giant Zeeman spin splitting and the spin-dependent electron scattering by polarized magnetic ions. If instead of the spin-up subband the spin-down subband is preferentially occupied the current direction is reversed.

to 22 K disappears and the photocurrent becomes almost independent of the sample temperature (Fig. 2(b)). The  $T$ -dependence under high power excitation is shown in Fig. 3. The signal is about constant for  $T < 100 \text{ K}$  and at higher temperatures it decreases with rising  $T$ . The signals in our pulse measurements are substantially higher than that at low power. As a result we obtain measurable signals at higher  $T$  as well as in the reference non-magnetic sample C (Fig. 3). It is remarkable that at high power excitation absolute values and the temperature dependences of the DMS sample B and the reference sample C are very similar to each other. This fact indicates that the presence of  $\text{Mn}^{2+}$  ions does not contribute to the current at this experimental conditions (high power excitation). Note, that the temperature dependence in Fig. 3 is also similar to that previously reported for non-magnetic semiconductors [6].

We now turn to microscopic mechanisms responsible for photocurrent generation. In case of Drude absorption, photocurrents stem from spin-dependent asymmetry of the optical transitions accompanied by scattering and/or from energy relaxation [6]. Here we focus on the energy relaxation of electron gas heated by THz yielding a polarization independent photocurrent. While the first mechanism depends on the radiation polarization the latter one is polarization independent. Investigating photocurrent in DMS at low temperature we do

not observe any polarization dependence. Therefore, the spin separation mechanism of interest here is based on the electron heating by THz radiation followed by energy relaxation. Usually, energy relaxation is considered to be spin-independent. However, in gyrotropic media, like CdTe- and (Cd,Mn)Te-based QWs investigated here, the spin-orbit interaction adds an asymmetric term to the scattering matrix element. This term is proportional to  $\sigma_\alpha(k_\beta + k'_\beta)$ , where  $\sigma$  is the vector composed of the Pauli matrices,  $\mathbf{k}$  and  $\mathbf{k}'$  are the initial and scattered electron wave vectors. Therefore, energy relaxation processes became spin-dependent. This is indicated for both spin subbands by bent arrows of different thicknesses in Fig. 4. The asymmetry of the electron-phonon interaction results in the spin current: The oppositely directed electron fluxes in two spin subbands,  $\dot{\mathbf{i}}_{\pm 1/2}$ , are of equal strength and the total charge current is zero,  $\mathbf{j} = e(\dot{\mathbf{i}}_{+1/2} + \dot{\mathbf{i}}_{-1/2}) = 0$ . Here  $e$  is the electron charge. Nevertheless, a finite pure spin current  $\mathbf{J}_s = (\dot{\mathbf{i}}_{+1/2} - \dot{\mathbf{i}}_{-1/2})/2$  is generated. This leads to a spatial spin separation and spin accumulation at the sample edges.

The application of an external magnetic field introduces an imbalance between the fluxes  $\dot{\mathbf{i}}_{\pm 1/2}$  giving rise to a net electric current  $\mathbf{j} = e(\dot{\mathbf{i}}_{+1/2} + \dot{\mathbf{i}}_{-1/2})$ . An obvious mechanism of the magnetic field induced imbalance of the oppositely directed spin flows, also relevant for non-magnetic semiconductors, is related to the Zeeman splitting of electron states [6]. This process is sketched in Fig. 4. Indeed, the fluxes  $\dot{\mathbf{i}}_{\pm 1/2}$  depend on the free carrier densities in the spin-up and spin-down subbands,  $n_{\pm 1/2}$ . Therefore, in a Zeeman spin-polarized system, where  $n_{+1/2} \neq n_{-1/2}$ , the fluxes  $\dot{\mathbf{i}}_{\pm 1/2}$  do no longer compensate each other yielding a net electric current. In DMS the electron Zeeman splitting is greatly enhanced due to the exchange interaction between free electrons and Mn<sup>2+</sup> ions. In the case of a low electron spin polarization, the equilibrium electron spin per electron is given by  $s = -E_Z/(4\bar{E})$  and the net current caused by the Zeeman splitting is given by (see Appendix I)

$$\mathbf{j}_Z = -4e \frac{E_Z}{4\bar{E}} \left( n_e \frac{\partial \mathbf{J}_s}{\partial n_e} \right), \quad (2)$$

where  $\bar{E}$  is a characteristic electron energy, which is equal to  $E_F$  for the degenerated electron gas and  $k_B T$  for the non-degenerated gas. The spin current is considered here as a function of the carrier density  $n_e$ . In particular, for the Boltzmann statistics, where  $\mathbf{J}_s \propto n_e$  and  $n_e \partial \mathbf{J}_s / \partial n_e = \mathbf{J}_s$ , Eq. (2) yields

$$\mathbf{j}_Z = -e \frac{E_Z}{k_B T} \mathbf{J}_s, \quad (3)$$

For the Fermi distribution, the derivative  $\partial \mathbf{J}_s / \partial n_e$  vanishes if the spin current is caused solely by  $\mathbf{k}$ -linear terms in the matrix element of the electron-phonon interaction

and is non-zero if higher order in  $\mathbf{k}$  terms contribute to the spin current.

Equations (2) and (3), showing that  $j_Z \propto E_Z$ , explain together with Eq. (1) the most striking experimental result: The sign inversion of the photocurrent with decreasing temperature. Indeed, at high temperatures the last term in Eq. (1) vanishes and only the intrinsic Zeeman splitting is responsible for the effect. The temperature decrease results in the giant Zeeman splitting whose sign is opposite to the intrinsic one. Thus, the direction of the photocurrent determined by the sign  $E_Z$  reverses.

This mechanism alone, however, does not explain the quantitative change of the current magnitude. It follows from the comparison of the temperature dependences of the Zeeman splitting of the electron subbands, estimated from the PL data and the photocurrents. Indeed, for sample B at  $B = 3$  T and  $T = 4.2$  K, the value of the giant Zeeman splitting is 2.6 meV. It exceeds by an order of magnitude the intrinsic Zeeman splitting of 0.25 meV. Whereas comparing the data obtained at the same magnetic field for 22 K, where only the intrinsic effect is present [16], and 4.2 K we get that the current strength changes much stronger, by a factor of about 40 (see Fig. 2). This variation of the signal is caused by Mn-related spin-dependent properties of DMS only and is much larger than that of the Zeeman splitting [19].

The mechanism, resulting in additional contribution to the conversion of the spin separation into the net current, is specific for DMS and is caused by the well known spin-dependent electron scattering by polarized magnetic ions [8]. In external magnetic fields, when the Mn ions are spin polarized, the scattering rate of electrons with the spins aligned parallel and antiparallel to the Mn spins becomes different [11]. This results in two different momentum relaxation times,  $\tau_{p,+1/2}$  and  $\tau_{p,-1/2}$ , in the spin subbands. Since the electron fluxes  $\dot{\mathbf{i}}_{\pm 1/2}$  are proportional to  $\tau_{p,\pm 1/2}$ , the polarization of Mn spins leads to a net electric current,  $\mathbf{j}_{Sc}$ . To obtain  $\mathbf{j}_{Sc}$  we assume that the momentum relaxation of electrons is governed by their interaction with Mn ion localized in QW. The corresponding Hamiltonian [8] is given by

$$H_{e-Mn} = \sum_i [u - \alpha (\mathbf{S}_i \cdot \boldsymbol{\sigma})] \delta(\mathbf{r} - \mathbf{R}_i), \quad (4)$$

where  $i$  is the Mn ion index,  $\mathbf{S}_i$  the vector composed of the matrices of the angular momentum 5/2,  $u\delta(\mathbf{r} - \mathbf{R}_i)$  the scattering potential without exchange interaction,  $\mathbf{r}$  the electron coordinate, and  $\mathbf{R}_i$  the Mn ion position. The electron scattering by the Mn potential determined by  $u$  is usually stronger than the exchange scattering determined by  $\alpha$ . Note, that the parameter  $\alpha$  in Eq. (4) is also responsible for the giant Zeeman splitting in Eq. (1). Then, for the case of  $|\alpha| \ll |u|$ , we derive (see Appendix II)

$$\mathbf{j}_{Sc} = 4e \frac{\alpha}{u} \mathbf{J}_s S_{Mn}, \quad (5)$$

where  $S_{Mn}$  is the average Mn spin along the magnetic field direction. We note that at low temperatures when DMS properties dominate the photocurrent both  $\mathbf{j}_{Sc}$  and  $\mathbf{j}_Z$  have the same direction because the average electron spin caused by the Zeeman effect is parallel to  $\mathbf{S}_{Mn}$ . The total electric current is given by the sum of both contributions  $\mathbf{j} = \mathbf{j}_Z + \mathbf{j}_{Sc}$ . In the case of a full spin polarized electron gas due to Zeeman effect, which can be achieved in DMS in reasonable magnetic fields, the electron flow in one of the spin subbands vanishes. Therefore, the electric current becomes independent of the magnetic field strength and carrier statistics and is given by  $\mathbf{j} = \mp 2e\mathbf{J}_s$ , where  $\mp$  corresponds to  $\pm$  sign of the Zeeman splitting.

To summarize, the electron gas heating in low-dimensional diluted magnetic semiconductors results in the generation of the pure spin current and correspondingly in the zero-bias spin separation. We show experimentally and theoretically that the carrier exchange interaction with localized magnetic spins in DMS giantly amplifies the conversion of the spin current into the electrical current. Two mechanisms are responsible for that, the giant Zeeman splitting of the conduction band states and the spin-dependent carrier scattering by localized Mn spins polarized by an external magnetic field. In weak magnetic fields for a degenerated electron gas the scattering mechanism dominates the current conversion.

We thank L. V. Litvin, E. L. Ivchenko, L. E. Golub, S. N. Danilov, N. S. Averkiev, and Yu. G. Semenov. The financial support from the DFG, RFBR, Polish Ministry of Science and Higher Education and Foundation for Polish Science is gratefully acknowledged.

## Appendix I

The electric current caused by different population of the spin-up and spin-down subbands in the magnetic field is given by

$$\begin{aligned} \mathbf{j}_Z &= e[\mathbf{i}_{+1/2}(n_e/2 + \delta n) + \mathbf{i}_{-1/2}(n_e/2 - \delta n)] \quad (\text{A1}) \\ &\approx e \left[ \mathbf{i}_{+1/2}(n_e/2) + \mathbf{i}_{-1/2}(n_e/2) + \delta n \frac{\partial(\mathbf{i}_{+1/2} - \mathbf{i}_{-1/2})}{\partial(n_e/2)} \right], \end{aligned}$$

where the fluxes  $\mathbf{i}_{\pm 1/2}$  are considered here as functions of the electron densities in the spin subbands,  $n_e$  is the total carrier density, and  $\delta n = sn_e$ . Since in zero magnetic field the electric current vanishes, i.e.,  $\mathbf{i}_{+1/2}(n_e/2) = -\mathbf{i}_{-1/2}(n_e/2)$ , the spin current is defined by  $\mathbf{J}_s(n_e) = 1/2[\mathbf{i}_{+1/2}(n_e/2) - \mathbf{i}_{-1/2}(n_e/2)]$ , and  $s = -E_Z/(4\bar{E})$ , we derive

$$\mathbf{j}_Z = -e \frac{E_Z}{k_B T} \mathbf{J}_s. \quad (\text{A2})$$

## Appendix II

The electric current contribution caused by difference in the momentum relaxation times  $\tau_{p,\pm 1/2}$  in the magnetic field is given by

$$\mathbf{j}_{Sc} = e \left( \mathbf{i}_{+1/2}^{(0)} \frac{\tau_{p,+1/2}}{\tau_p^{(0)}} + \mathbf{i}_{-1/2}^{(0)} \frac{\tau_{p,-1/2}}{\tau_p^{(0)}} \right), \quad (\text{A3})$$

where  $\mathbf{i}_{\pm 1/2}^{(0)}$  and  $\tau_p^{(0)}$  are the electron fluxes and relaxation time in zero field, respectively. For the electron scattering by polarized Mn impurities, the times  $\tau_{p,\pm 1/2}$  assume the form

$$\frac{\tau_{p,\pm 1/2}}{\tau_p^{(0)}} = \frac{\sum_{J=-5/2}^{+5/2} |u \mp \alpha J|^2 / 6}{\sum_{J=-5/2}^{+5/2} |u \mp \alpha J|^2 f_{Mn}(J)} \approx \left[ 1 \pm 2 \frac{\alpha}{u} S_{Mn} \right], \quad (\text{A4})$$

where  $f_{Mn}(J)$  is the distribution function of Mn spin projections along the magnetic field, and  $S_{Mn} = \sum_{J=-5/2}^{+5/2} J f_{Mn}(J)$  is the average Mn spin. Then, one obtains for the electric current

$$\mathbf{j}_{Sc} = 2e \frac{\alpha}{u} S_{Mn} (\mathbf{i}_{+1/2}^{(0)} - \mathbf{i}_{-1/2}^{(0)}) \approx 4e \frac{\alpha}{u} \mathbf{J}_s S_{Mn}. \quad (\text{A5})$$

- 
- [1] *Spin Physics in Semiconductors*, Ed. M. I. Dyakonov (Springer, Berlin, 2008).
  - [2] J. Fabian, A. Matos-Abiague, C. Ertler, P. Stano, and I. Zutic, *Acta Phys. Slov.* **57**, 565 (2007), arXiv:0711.1461 (2007).
  - [3] R. D. R. Bhat, F. Nastos, A. Najmaie, and J. E. Sipe, *Phys. Rev. Lett.* **94**, 096603 (2005).
  - [4] S. A. Tarasenko and E. L. Ivchenko, *JETP Lett.* **81**, 231 (2005).
  - [5] H. Zhao, X. Pan, A.L. Smirl, R. D. R. Bhat, A. Najmaie, J. E. Sipe, and H. M. van Driel, *Phys. Rev. B* **72**, 201302 (2005).
  - [6] S. D. Ganichev, V. V. Bel'kov, S. A. Tarasenko, S. N. Danilov, S. Giglberger, Ch. Hoffmann, E. L. Ivchenko, D. Weiss, W. Wegscheider, Ch. Gerl, D. Schuh, J. Stahl, J. De Boeck, G. Borghs, and W. Prettl, *Nature Phys.* **2**, 609 (2006).
  - [7] T. Dietl, in *Handbook on Semiconductors*, vol. 3b, Ed. T. S. Moss (North-Holland, Amsterdam, 1994).
  - [8] J. K. Furdyna, *J. Appl. Phys.* **64**, R29 (1988).
  - [9] C. Gorini, P. Schwab, M. Dzierzawa, and R. Raimondi, *Phys. Rev. B* **78**, 125327 (2008).
  - [10] S. A. Crooker, D. A. Tulchinsky, J. Levy, D. D. Awschalom R. Garcia and N. Samarth, *Phys. Rev. Lett.* **75**, 505 (1995).
  - [11] J. C. Egues and J. W. Wilkins, *Phys. Rev.* **58**, R16012 (1998).
  - [12] J. Jaroszynski, T. Andreczyk, G. Karczewski, J. Wróbel, T. Wojtowicz, E. Papis, E. Kaminska, A. Piotrowska, D. Popovic, and T. Dietl, *Phys. Rev. Lett.* **89**, 266802 (2002).

- [13] M. K. Kneip, D. R. Yakovlev, M. Bayer, G. Karczewski, T. Wojtowicz, and J. Kossut, *Appl. Phys. Lett.* **88**, 152105 (2006).
- [14] D. Keller, G. V. Astakhov, D. R. Yakovlev, L. Hansen, W. Ossau, and S.A. Crooker, NATO Science Series II, vol. 19 *Optical Properties of 2D Systems with Interacting Electrons*, Eds. W. J. Ossau and R. Suris (Kluwer Academic Publishers, 2003), pp. 217 - 232.
- [15] S. D. Ganichev and W. Prettl, *Intense Terahertz Excitation of Semiconductors* (Oxford University Press, Oxford, 2006).
- [16] We note the fact that the slopes of  $J_x(B)$  dependences detected for  $T$  of about 20 K are the same for low and high power excitations.
- [17] A. A. Sirenko, T. Ruf, M. Cardona, D. R. Yakovlev, W. Ossau, A. Waag, and G. Landwehr, *Phys. Rev. B* **56**, 2114 (1997).
- [18] D. Keller, D. R. Yakovlev, B. König, W. Ossau, Th. Gruber, A. Waag, L. W. Molenkamp, and A. V. Scherbakov, *Phys. Rev. B* **65**, 035313 (2002).
- [19] Our experiments under conditions where Mn plays no essential role (reference non-magnetic sample and DMS samples at high power excitation) demonstrate that the photocurrent due to intrinsic effect is almost independent of temperature for  $T < 100$  K (see Fig. 3).